Retinal Structure and Function in Perinatally HIV-Infected and cART-Treated Children: A Matched Case–Control Study

Nazli Demirkaya,[1] Sophie Cohen,[2] Ferdinand W. N. M. Wit,[3,4] Michael D. Abramoff,[5–7] Reinier O. Schlingemann,[1,8] Taco W. Kuijpers,[2] Peter Reiss,[3,4,9] Dasja Pajkrt,[2] and Frank D. Verbraak[1,10]

[1]Department of Ophthalmology, Academic Medical Center, University of Amsterdam, Amsterdam, The Netherlands
[2]Department of Pediatric Hematology, Immunology, and Infectious Diseases, Emma Children's Hospital, Academic Medical Center, University of Amsterdam, Amsterdam, The Netherlands
[3]Department of Global Health, Academic Medical Center, University of Amsterdam, and Amsterdam Institute for Global Health and Development, Amsterdam, The Netherlands
[4]Department of Internal Medicine, Division of Infectious Diseases, Center for Infection and Immunity Amsterdam (CINIMA), Academic Medical Center, Amsterdam, The Netherlands
[5]Department of Ophthalmology and Visual Sciences, Stephen A. Wynn Institute for Vision Research, University of Iowa, Iowa City, Iowa, United States
[6]Department of Biomedical Engineering and Department of Electrical and Computer Engineering, University of Iowa, Iowa City, Iowa, United States
[7]Iowa City Veterans Administration Medical Center, Iowa City, Iowa, United States
[8]Netherlands Institute for Neuroscience, Royal Netherlands Academy of Arts and Sciences, Amsterdam, The Netherlands
[9]HIV Monitoring Foundation, Amsterdam, The Netherlands
[10]Department of Biomedical Engineering and Physics, Academic Medical Center, University of Amsterdam, Amsterdam, The Netherlands

Correspondence: Nazli Demirkaya, Department of Ophthalmology, Academic Medical Center, PO Box 22660, 1100 DD, Amsterdam, The Netherlands; Ndemirkaya@amc.nl.

Submitted: March 12, 2015
Accepted: April 30, 2015

Citation: Demirkaya N, Cohen S, Wit FWNM, et al. Retinal structure and function in perinatally HIV-infected and cART-treated children: a matched case–control study. *Invest Ophthalmol Vis Sci*. 2015;56:3945–3954. DOI:10.1167/iovs.15-16855

Purpose. Subtle structural and functional neuroretinal changes have been described in human immunodeficiency virus (HIV)–infected adults without retinitis treated with combination antiretroviral therapy (cART). However, studies on this subject in HIV-infected children are scarce. This study aimed to assess the presence of (neuro)retinal functional and structural differences between a group of perinatally HIV-infected children on cART and age-, sex-, ethnicity-, and socioeconomically matched healthy controls.

Methods. All participants underwent an extensive ophthalmological examination, including functional tests as well as optical coherence tomography, to measure individual retinal layer thicknesses. Multivariable mixed linear regression models were used to assess possible associations between HIV status (and other HIV-related parameters) and ocular parameters, while accounting for the inclusion of both eyes and several known confounders.

Results. Thirty-three HIV-infected children (median age 13.7 years [interquartile range (IQR), 12.2–15.8], median $CD4^+$ T-cell count 760 cells/mm^3, 82% with an undetectable HIV viral load [VL]), and 36 controls (median age 12.1 years [IQR, 11.5–15.8]) were included. Contrast sensitivity (CS) was significantly lower in the HIV-infected group (1.74 vs. 1.76 logCS; $P = 0.006$). The patients had a significantly thinner foveal thickness (−11.2 μm, $P = 0.012$), which was associated with a higher peak HIV VL (−10.3 μm per log copy/mL, $P = 0.016$).

Conclusions. In this study, we found a decrease in foveal thickness in HIV-infected children, which was associated with a higher peak VL. Longitudinal studies are warranted to confirm our findings and to determine the course and clinical consequences of these foveal changes.

Keywords: HIV, SD-OCT, visual function, children, retinal layer thickness

The spectrum of human immunodeficiency virus (HIV)–related retinal disease has changed drastically since the introduction of combination antiretroviral therapy (cART), with a major decline in incidence of opportunistic infections, such as cytomegalovirus (CMV) retinitis, as well as noninfectious ischemic HIV retinopathy.

However, even in cART-treated individuals with well-suppressed HIV infection and absence of opportunistic infections, functional and structural retinal abnormalities have been reported, such as a subtle loss of color vision and/or contrast sensitivity, visual field deficits, and a thinner retinal nerve fiber layer (RNFL) thickness.[1–10] These changes are thought to be part of a "HIV-associated neuroretinal disorder" (HIV-NRD) and may be mediated by several processes, such as longstanding microvasculopathy,[11–17] direct damage of neural tissue by HIV and/or cART,[18–20] and chronic (para)inflammation.[21]

It is unclear whether such retinal changes are also present in cART-treated HIV-infected children (without a history of ocular opportunistic infections). So far, one study group has addressed this question and reported a thinning of the peripapillary RNFL

in 19 HIV-infected children as compared to 21 healthy controls,[22] as well as foveal thickening and multifocal electroretinographical (mf-ERG) abnormalities in a smaller subgroup of HIV-infected children.[23]

This study is part of an interdisciplinary observational cross-sectional study, evaluating neurological and neurocognitive disorders, neuroimaging, and ophthalmic alterations in perinatally HIV-1-infected children in The Netherlands.[24] In the current study, we assessed the presence of retinal structural and functional differences between perinatally HIV-infected children on cART and a group of age-, sex-, ethnicity-, and socioeconomically matched healthy controls. This is the first study employing the Iowa Reference Algorithm[25,26] on spectral-domain optical coherence tomography (SD-OCT) scans in HIV-infected children, enabling the measurement of the thickness of individual retinal layers.

Subjects and Methods

The study adhered to the tenets of the Declaration of Helsinki, and approval was obtained from the investigational review board at the Academic Medical Center in Amsterdam. Written informed consent was obtained from all parents and from children aged 12 and above.

Study Participants

All HIV-infected children between 8 and 18 years of age attending the pediatric HIV outpatient clinic of the Academic Medical Center were approached for study participation between December 2012 and January 2014. Healthy controls were recruited through parental evenings at schools, sports clubs, and churches situated in areas in Amsterdam, aiming to capture an ethnically diverse population with a lower socioeconomic status (SES) than the general Dutch population, as similar as possible to patients.[27] Exclusion criteria were chronic (non–HIV-associated) neurological diseases like epilepsy, (history of) intracerebral neoplasms, and psychiatric disorders. Intelligence quotient (IQ) was measured using the WISC III and WAIS III for children older than 16 years of age.[28,29] Frequency matching for age, sex, ethnicity, and SES was performed. Socioeconomic status was determined using parental education and occupational status. Parental education was scored according to the International Standard Classification of Education (ISCED). Occupational status was defined as no, one, or two caregivers with a paid job. The remaining sociodemographic data were obtained using standardized questionnaires.

HIV- and cART-Related Characteristics

Historical HIV viral load (VL) and $CD4^+$ T-cell counts, Centers for Disease Control (CDC) clinical stage category, and cART treatment history were derived from the Dutch HIV Monitoring Foundation database.[30] Clinical, immunological, and virological data prior to migration to The Netherlands were collected for the immigrant children and registered as "missing" when not traceable. Outpatient visits in our center occur every 3 months, and all clinical, immunological, and virological data are registered by the HIV Monitoring Foundation. The time of HIV diagnosis was defined as the first known documented positive HIV test, also using test data from the country of origin of children who were born outside The Netherlands. Viral load results were based on different assays used between 1995 and 2013 with decreasing detection limits (<1000 copies/mL in 1995 to <40 copies/mL in 2013). An undetectable HIV VL was defined as a VL below the detection limit of the assay used at that time. The HIV VL during study participation was determined by the Abbott (Chicago, IL, USA) Real Time HIV-1 assay. The peak HIV VL was defined as the highest VL prior to cART initiation, or the highest HIV VL due to interruption of cART or virological failure. The proportion of life spent with a detectable VL was calculated by adding all days between two detectable HIV VL and half of the days between the last detectable and the next undetectable HIV VL, and dividing the cumulative number of days with a detectable VL by the participant's age at inclusion into this study.

To account for physiological age-related differences in CD4+ T-cell counts, all registered $CD4^+$ T-cell counts were transformed into z scores by subtracting the reference value for the age at the time of the $CD4^+$ T-cell measurement and dividing this by the age-related SD. A z score of 0 represents the age-appropriate mean.[30] The nadir $CD4^+$ T-cell z score was defined as the lowest z score prior to cART initiation or to a maximum of 3 months after the start of cART. At inclusion, absolute $CD4^+$ T-cell counts were analyzed instead of z scores, as all children were >8 years of age. Lastly, we calculated the cumulative time with a $CD4^+$ T-cell count below 50, 100, 200, 350, and 500 cells/mm^3 by adding all days between two $CD4^+$ T-cell measurements of <500 cells/mm^3 to half of the days between two $CD4^+$ T-cell measurements with one <500 cells/mm^3 and one >500 cells/mm^3.

Ophthalmic Examination

Ophthalmic exclusion criteria were high refractive errors (spherical equivalent [SE] > +5.5 or > −8.5 diopters [D]), visual acuity below 0.1 logMAR, intraocular pressure (IOP) higher than 21 mm Hg, significant media opacities, and a history of ocular surgery or ocular disease. One patient with a history of CMV retinitis in both eyes and one control with a refractive error > +5 D were excluded for not meeting the inclusion criteria. In addition, two left eyes of two HIV-infected children were excluded from analysis due to the presence of uveitis and congenital toxoplasmosis lesions, respectively.

Visual acuity (VA) was measured using a modified Early Treatment Diabetic Retinopathy Study (ETDRS) chart with Sloan letters (Lighthouse, New York, NY, USA) at 4 m. Visual acuity was recorded in logMAR units. Intraocular pressure was measured by air-puff tonometry (computerized tonometer, CT80; Topcon Medical Systems, Inc., Oakland, NJ, USA). All subjects underwent pupil dilation (0.5% tropicamide and 5% phenylephrine) and a standard ophthalmic examination, including slit-lamp biomicroscopy with a handheld lens, as well as fundus photography.

Mars Contrast Sensitivity (CS) Charts

All children were tested with the Mars Letter Contrast Sensitivity Test (Mars Perceptrix, Chappaqua, NY, USA), a portable chart measuring 23 × 36 cm, consisting of 48 letters arranged in eight rows of six Sloan letters each. The Mars test letters subtend 2° (at 50 cm), the change in contrast between successive letters is 0.04 log units, and the contrast range is from 0.04 to 1.92 log units. The Mars test has test–retest reliability equal to or better than the Pelli Robson test and has proven to be a useful and practical alternative to the Pelli Robson contrast sensitivity chart.[23,31–34]

Lanthony D-15 Color Vision Panel Test

Color vision was determined using the Lanthony Desaturated 15-hue (D-15) color vision test.[35] This test is more sensitive to subtle color discrimination deficiencies and is easier to perform and score than the Farnsworth-Munsell 100-hue test

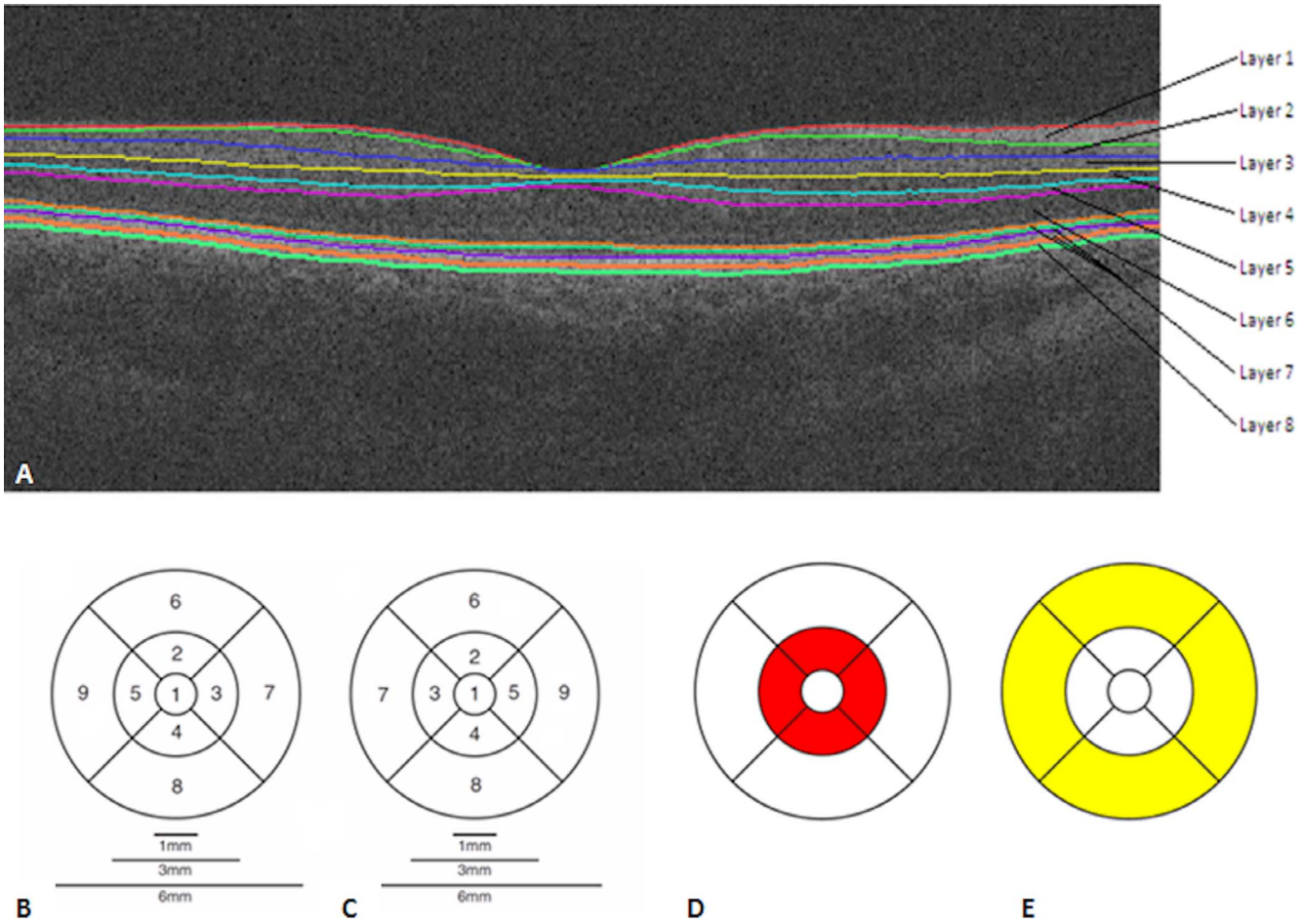

FIGURE 1. (**A**) Macular SD-OCT B-scan with intraretinal surfaces as indicated by the *colored lines* and segmented using the Iowa Reference Algorithm.[25,26] In this study, the highly reflective layer between inner and outer segments and the outer segments up to the retinal pigment layer were taken together as one layer, the outer segment layer (OSL), ignoring the line ascribed to the cone outer segments.[63] Corresponding retinal layers: 1, retinal nerve fiber layer, 2, ganglion cell layer, 3, inner plexiform layer, 4, inner nuclear layer, 5, outer plexiform layer, 6, outer nuclear layer + inner segments (photoreceptors), 7, outer segments (photoreceptors), 8, retinal pigment epithelium. (**B**–**E**) ETDRS grid. Nine subfields of the nine ETDRS regions in each eye. (**B**) Right eye. (**C**) Left eye. For each retinal layer, three areas were defined using this ETDRS grid: the fovea, the central circle with a diameter of 1 mm (depicted as 1 in [**B**, **C**]); the pericentral ring, a donut-shaped ring centered on the fovea with an inner diameter of 1 mm and an outer diameter of 3 mm (**D**); and the peripheral ring, with an inner diameter of 3 mm and outer diameter of 6 mm (**E**). Thickness measurements of the pericentral and peripheral rings were estimated by averaging the thickness measurements of the four corresponding quadrant areas (segments 2–5 for the pericentral ring and segments 6–9 for the peripheral ring).

(FM-100).[36] Testing was performed under standard illuminant conditions and repeated once when errors were made. Color confusion index (CCI), as described by Vingrys and King-Smith,[37] was determined for each eye. Errorless performance is scored with a CCI of 1.0, and higher values indicate a worse test result. The best outcome per eye was used for analysis.

Rarebit Perimetry and Rarebit Fovea Test

The Rarebit Perimetry (RBP) and Rarebit Fovea Test (RFT) are visual function tests developed to detect subtle central visual field damage and have been described extensively elsewhere.[38,39] The RBP (inner and outer tests) evaluates the central 30° visual field, while the RFT evaluates the central 4° visual field. The results of the Rarebit test are presented as mean hit rate (MHR), a percentage of the stimuli seen by the subject.

SD-OCT and Retinal Layer Segmentation

Optical coherence tomography images of the subjects were obtained with SD-OCT (Topcon 3D OCT-1000; Topcon, Inc., Paramus, NJ, USA) using the 3D macular and disc volume scan protocols. Only high-quality images with a Topcon image quality factor (QF) > 60 were used. From each 3D macular volume, individual retinal layers were segmented automatically by the Iowa Reference Algorithm,[25,26] which uses an extensively validated, robust, fully three-dimensional graph search approach (Fig. 1A). The Iowa Reference Algorithm[25,26] allows for calculation of the thickness of all individual retinal layers for each of the nine ETDRS grid defined regions (Figs. 1B–E).

In addition, peripapillary RNFL thickness measurements were acquired from the 3D optic nerve head OCTs using the same Iowa Reference Algorithm.[25,26] The peripapillary ring was centered manually if needed, with the center of the ring coinciding with the center of the optic disc.

Statistical Analysis

Demographic characteristics were compared between groups using the unpaired *t*-test, the Mann-Whitney *U* test, or the χ^2 test. Univariable and multivariable linear regression models with mixed effects were used to explore associations between HIV status and ocular variables in all study participants while accounting for the inclusion of both eyes and potential confounders (age at study visit,[40–44] sex,[41–43] IQ [corrected for in the function test analyses], OCT QF,[40,44–46] and SE[44,47] [corrected for in the OCT analyses]). Covariates with a *P* value < 0.2 in univariable analysis were incorporated in the multivariable models. In the multivariable models the level of significance was set at a *P* value $<$ 0.05.

The outcome variables that were significantly different between HIV-infected and healthy children in the models described above were further investigated in the HIV-infected group only, again using multivariable mixed linear regression models. Associations between the specified parameters and (1) disease-related factors (HIV VL at time of study visit, peak HIV VL, the proportion of life spent with a detectable VL, nadir $CD4^+$ T-cell *z* score, duration of $CD4^+$ T-cell counts $<$ 500 cells/mm^3, CDC clinical category) and (2) cART-related factors (age at cART initiation, duration of cART use, current cART use, and duration of exposure to didanosine and/or stavudine (which can cause a toxic retinopathy[48–50]) were explored.

Furthermore, possible correlations between visual function test results and retinal layer thickness were assessed, in particular, focusing on the significant parameters.

Data entry and management was performed using OpenClinica open source software (Waltham, MA, USA). Statistical analyses were carried out using Stata Statistical Software, release 12 (StataCorp LP, College Station, TX, USA).

Results

Demographic and Clinical Characteristics

Table 1 shows the demographic and clinical characteristics of all study participants. In total, 33 HIV-infected children (median age 12.1; interquartile range [IQR], 11.5–15.8) and 36 healthy controls were included (median age 13.7; IQR, 12.2–15.8). Most children were of black (HIV: 79%; healthy: 75%) or mixed black (HIV: 12%; healthy: 17%) ethnicity. Although mean SE, IOP, and VA differed significantly between the two groups, all values were within a normal range. Among the HIV-infected children, 32 (97%) had ever received cART, and 28 (85%) were using cART at time of the study assessment; among these, 27 (96%) had an undetectable plasma HIV VL. The median $CD4^+$ T-cell count was 760 cells/mm^3 at the time of assessment.

Visual Function Tests

No significant differences in color vision and central visual field were detected between the two groups (Table 2). Contrast sensitivity was significantly lower in the HIV-infected children, although the difference was only half a letter (1.74 vs. 1.76 logCS, *P* value = 0.006).

Thickness of Individual Retinal Layers

Multivariable mixed linear regression analyses (adjusted for age, sex, OCT QF, and SE) were performed to detect differences between the HIV-infected and healthy groups. Mean retinal layer thicknesses (individual retinal layers, peripapillary RNFL, and total retinal thickness) for patients and controls are shown in Table 3. Human IV-infected children had a significantly thinner total foveal thickness (–11.2 μm, *P* value = 0.012), predominantly due to a thinner foveal outer nuclear layer and inner segments (ONL-IS; –6.2 μm, *P* value = 0.011).

Multivariable Analyses Within the HIV-Infected Group

Visual function and OCT parameters that differed significantly between HIV-infected and healthy children were further investigated in the HIV-infected group to identify potential associations between these parameters and HIV- and/or cART-related variables.

Multivariable mixed regression analysis showed an inverse association between total foveal retinal thickness and peak HIV VL (–10.7 μm per log copy/mL, *P* value = 0.016, Fig. 2); a similar relationship was observed between the foveal ONL-IS and peak HIV VL (–7.1 μm per log copy/mL, *P* value = 0.013). No other associations were found between visual function, OCT parameters, and HIV- or cART-related parameters.

Structure–Function Relationships

Finally, we explored potential correlations between visual function test results (color vision, CS, and central visual field) and OCT retinal layer thickness in HIV-infected children. No associations were observed (data not shown).

Discussion

This study aimed to assess retinal structure and visual function in a group of perinatally HIV-infected children, compared to a group of matched healthy controls. Subtle structural retinal changes and visual dysfunction, termed HIV-associated neuroretinal disorder, have been described in HIV-infected adults on cART without infectious retinitis[1–10,14,16,17,51–59]; however, data on this subject in HIV-infected children are limited and derived from one study group.[22,23] This is the first study assessing individual retinal layer thicknesses and exploring associations between various HIV-and cART-related factors and ocular parameters in HIV-infected children.

Our findings indicate that HIV-infected children have a thinner foveal retinal thickness than healthy controls while having a comparable peripapillary RNFL thickness and visual function outcomes.

We found no significant differences in peripapillary RNFL thickness between HIV-infected children and age-, sex-, ethnicity- and socioeconomically matched controls, which is not in line with the previous pediatric study by Moschos et al.[22] They reported a thinner peripapillary RNFL thickness in a group of 19 HIV-infected children compared to a group of 21 age-matched healthy children.[22] Of note, however: In our study, we used spectral-domain OCT, which is more accurate in measuring retinal and RNFL thickness than time-domain OCT.[60] Furthermore, in our assessment of peripapillary RNFL thickness, we adjusted for known confounders such as age,[40–44] sex,[41–43] SE,[40,44,47] and OCT QF.[40,44,46] In addition, we applied multilevel mixed linear modeling to take correlations between right and left eyes into account.

In their second study, Moschos et al.[23] found an increase in foveal thickness as well as multifocal ERG abnormalities in a subgroup, consisting of 10 eyes (the number of children was not stated), in their cohort. We observed the opposite in our study, with a significantly lower total foveal thickness in the

Investigative Ophthalmology & Visual Science

Table 1. Participant Characteristics

Demographic Characteristics	HIV-Infected Children, *nr* = 33	Healthy Controls, *nr* = 36	*P* Value
Male sex	17 (52)	17 (47)	0.807
Age	12.1 (11.5 to 15.8)	13.7 (12.2 to 15.8)	0.170
Country of birth			
The Netherlands	10 (30)	34 (94)	
Sub-Saharan Africa	18 (55)	2 (6)	
Suriname	1 (3)	0 (0)	
Other	4 (12)	0 (0)	**<0.001**
Ethnicity			
Black	26 (79)	27 (75)	0.358
Mixed black	4 (12)	6 (17)	
Caucasian	0 (0)	3 (8)	
Other	3 (9)	0 (0)	
Education, child			
Primary school	9 (27)	19 (53)	**0.036**
High school	10 (30)	13 (36)	
Special school	9 (27)	1 (3)	
Other	5 (15)	3 (8)	
Country of birth, parent, M/F			
The Netherlands	1 (3)/4 (12)	6 (17)/8 (22)	**<0.001**
Sub-Saharan Africa	25 (76)/18 (55)	8 (22)/5 (14)	
Surinam	2 (6)/3 (9)	19 (53)/19 (53)	
Other	5 (15)/6 (18)	3 (8)/4 (11)	
ISCED educational level parent*	5 (4 to 6)	5 (5 to 6)	0.245
1 parent employed	16 (62)	24 (67)	0.468
2 parents employed	5 (19)	9 (25)	0.798

HIV- and cART-Related Characteristics	HIV-Infected Children, *nr* = 33	Healthy Controls, *nr* = 36	*P* Value
Clinical			
Age at HIV diagnosis, y	2.3 (0.7 to 4.9)	-	-
CDC category			
N	4 (12)	-	-
A	6 (18)	-	-
B	15 (46)	-	-
C	8 (24)	-	-
Cerebral HIV/AIDS†	2 (6)	-	-
$CD4^+$ T-cell and HIV viral load			
Peak HIV viral load, log copies/mL	5.54 (5.10 to 5.92)	-	-
Nadir $CD4^+$ *z* score	−0.7 (−1.4 to −0.4)	-	-
HIV viral load at eye exam			
Detectable	6 (18)	-	-
Undetectable	27 (82)	-	-
$CD4^+$ T-cell count at eye exam, $*10^6$/L	760 (580 to 950)	-	-
$CD4^+$ *z* score at eye exam	−0.1 (−0.3 to 0.2)	-	-
Time living with a detectable viral load, y	2.4 (1.4 to 5.8)	-	-
Time with $CD4^+$ T-cell count <500, $*10^6$/L, mo	18.3 (11.0 to 94.1)	-	-
cART			
Age at cART initiation, y	2.6 (1.0 to 6.2)	-	-
Current cART use	28 (85)	-	-
Duration cART use, y	10.7 (7.1 to 14.4)	-	-
Mono- or dual therapy treatment before cART	3 (9)	-	-
Duration of exposure to didanosine, y, *n* = 15	2.2 (0.8 to 4.4)	-	-
Duration of exposure to stavudine, y, *n* = 12	4.6 (3.9 to 5.6)	-	-

Investigative Ophthalmology & Visual Science

Table 1. Continued

Ocular Features	Mean ± SD, Range	Mean ± SD, Range	*P* Value
Spherical equivalent refraction, D	−0.86 ± 1.6 (−5.9 to 1.3)	−1.6 ± 2.2 (−7.1 to 0.8)	**0.033**
Intraocular pressure, mm Hg	14.1 ± 2.4 (10 to 19)	16.2 ± 3.1 (10 to 24)	**<0.001**
Visual acuity, logMAR	−0.02 ± 0.06 (−0.2 to 0.1)	−0.05 ± 0.05 (−0.18 to 0.06)	**0.008**
Topcon image quality factor, macula scan	85.6 ± 6.9 (60.0 to 100.6)	85.3 ± 7.2 (68.7 to 101.9)	0.771
Topcon image quality factor, disc scan	84.7 ± 7.2 (66.6 to 94.9)	86.0 ± 5.3 (73.6 to 96.5)	0.247

Values are expressed as *N* (%), median (IQR), or mean ± standard deviation (SD). *P* values in bold are $P < 0.05$. M/F, mother/father; *nr*, number of patients.

* Most educated parent.

† HIV encephalopathy ($n = 2$) and CMV encephalitis ($n = 1$).

group of HIV-infected children, predominantly due to a thinner ONL-IS of the photoreceptors as well as thinner inner retinal layers. Since we are the first group measuring individual OCT retinal layer thicknesses in HIV-infected children, comparison of our findings to other studies in children is not yet attainable. In HIV-infected adults, however, it is thought that damage (caused by HIV and/or other factors) to the optic nerve leads to thinning of the peripapillary RNFL.[1,7,9] Multiple adult studies indeed reported a decrease in peripapillary RNFL thickness, particularly in patients with (a history of) low (<100 cells/mm^3) CD4$^+$ T-cell counts.[4,52,57–59] Since the axons of the ganglion cell layer make up the optic nerve in large part, a decrease in peripapillary RNFL implies that a decrease in ganglion cell layer thickness (and possibly other inner retinal layers) would also be expected, but no study has reported on this. If we extrapolate this hypothesis of HIV-associated neuroretinal degeneration to HIV-infected children, a decrease of peripapillary RNFL thickness and inner retinal layers (especially in the pericentral retinal area, where the ganglion cell layer is thickest) would be expected in this group. Surprisingly, we detected a thinner foveal thickness and no other OCT differences in the HIV-infected children as compared to the controls.

However, the consequences of chronic HIV infection in perinatally infected children are likely to be different from those in adults because their infection occurs during rather than after (neuronal) development. This may result in different findings between adults and children. Of all foveal layers, the outer nuclear layer shows the most distinct increase during foveal maturation (from infancy to 16 years of age), creating a bulge.[61] Therefore, if we speculate that HIV infection may interrupt this maturation, this would be mostly reflected in the outer nuclear layer. This may explain the significantly thinner fovea—in particular, the ONL-IS—that we detected in the HIV-infected children in our study. Supporting this hypothesis was the significant association we observed between a higher peak HIV VL and thinner foveal ONL-IS.

A recent study in 22 perinatally HIV-infected children (median age 16.6 years) on cART, with nadir CD4 counts > 200 cells/mm^3, reported an absence of vision-threatening disease but a high prevalence (18%) of strabismus,[62] which is thought to be a developmental disorder, again suggesting that HIV infection may hamper the development of the visual system.

We did not detect any correlations between retinal structure and visual function in HIV-infected children. This was to be expected considering the high interindividual variability in retinal layer thickness and functional test outcomes and the small changes observed.

Strengths of our study are the inclusion of an age-, sex-, ethnicity-, and socioeconomically matched control group and the adjustment for relevant potentially confounding factors in our statistical analyses. Of note, we found IQ to be an important confounder when analyzing the functional test outcomes, with a strong positive association between test results and total IQ. Nonetheless, there are some limitations. Even though this is the largest ophthalmological study in clinically stable HIV-infected children without retinitis at present, the relatively small sample size may have hampered the detection of some potential associations. Secondly, a cross-sectional study of parameters known to have a high interindividual variability is less able to detect small changes in retinal structure and function than a longitudinal study.

Although we aimed to capture a control population as similar as possible to the patients by matching for age, sex, and SES, there is a possibility that some of the variability in the results we detected was caused by non–HIV-related factors.

The visual function tests we used are psychophysical techniques and involve an element of subjectivity; however, we used standardized protocols (i.e., lightning conditions, testing distance) to minimize this problem. A more objective

Table 2. Visual Function Test Results in HIV Patients and Controls

	HIV-Infected Children, *nr* = 33				Healthy Controls, *nr* = 36					
Visual Function Test	*n*	Mean	SD	Range	*n*	Mean	SD	Range	Coefficient	*P* Value
Lanthony D15 test, CCI	64	1.18	0.23	1–2.12	70	1.15	0.19	1–1.87	−0.0379	0.315
Mars CS logCS	63	1.74	0.03	1.64–1.80	72	1.76	0.03	1.72–1.92	−0.0192	**0.006**
RBP outer test, MHR	60	79.5	13.3	47–99	71	83.8	11.6	43–100	−2.44	0.379
RBP inner test, MHR	60	93.6	11.1	44–100	72	94.8	7.4	63–100	0.0158	0.993
Rarebit Fovea Test, MHR	60	88.6	17.3	38–100	72	93.9	9.8	50–100	−2.0372	0.476

P values derived from multivariable linear mixed model and adjusted for age at assessment, sex, and total IQ. *P* value in bold is $P < 0.05$. *nr*, number of patients; *n*, number of eyes.

Table 3. OCT Individual Retinal Layer Thicknesses in HIV Patients and Controls

	HIV-Infected Children, *nr* = 33				Healthy Controls, *nr* = 36					
Macular Layer	***n***	**Mean**	**SD**	**Range**	***n***	**Mean**	**SD**	**Range**	**Coefficient**	***P* Value**
RNFL										
Fovea	64	3.4	1.5	0.8–8.5	70	4.0	1.8	1.1–11.3	−0.6162	0.068
Pericentral ring	64	20.3	1.8	15.6–24.7	70	21.3	1.9	15.6–25.1	−0.9317	**0.015**
Peripheral ring	64	33.1	3.4	24.1–42.7	70	34.3	3.3	26.5–41.0	−1.009	0.153
GCL										
Fovea	64	10.9	3.3	4.1–18.4	70	14.4	5.1	5.5–31.3	−3.1545	**0.001**
Pericentral ring	64	51.8	5.6	31.2–63.1	70	53.3	4.8	41.7–66.2	−2.0811	0.094
Peripheral ring	64	32.0	3.9	26.0–43.4	70	31.7	2.7	25.3–38.5	0.0480	0.951
IPL										
Fovea	64	20.3	3.8	14.0–29.9	70	22.1	4.4	14.5–31.2	−1.5397	0.103
Pericentral ring	64	39.6	3.5	33.9–49.9	70	40.4	3.0	34.1–46.7	−0.9592	0.217
Peripheral ring	64	40.6	3.5	31.4–49.3	70	40.4	2.7	34.9–47.7	−0.0580	0.937
INL										
Fovea	64	16.9	3.6	11.2–27.6	70	19.3	4.1	11.5–32.1	−1.9766	**0.026**
Pericentral ring	64	38.3	3.8	30.8–47.0	70	39.0	2.8	33.8–45.4	−0.9530	0.225
Peripheral ring	64	34.0	3.2	27.7–42.0	70	33.4	2.4	25.2–39.6	0.2916	0.656
OPL										
Fovea	64	23.6	4.4	14.7–37.4	70	23.2	4.0	15.0–33.3	0.4933	0.562
Pericentral ring	64	27.6	3.7	19.9–37.9	70	27.9	3.9	22.2–40.0	−0.2125	0.795
Peripheral ring	64	25.2	1.6	22.2–28.9	70	24.8	1.4	21.6–28.4	0.3330	0.309
ONL-IS										
Fovea	64	107.1	11.9	82.1–135.1	70	112.4	9.6	92.4–130.2	−6.2414	**0.011**
Pericentral ring	64	95.5	8.9	81.6–116.7	70	96.3	8.4	73.6–111.1	0.2998	0.507
Peripheral ring	64	81.7	6.9	70.0–96.6	70	82.8	5.6	70.4–94.9	−1.9953	0.311
OSL										
Fovea	64	50.9	2.6	44.5–56.8	70	49.0	3.9	29.6–54.5	1.8653	**0.010**
Pericentral ring	64	43.7	2.7	37.6–51.7	70	41.2	4.1	20.8–46.9	2.1511	**0.006**
Peripheral ring	64	38.8	2.8	32.7–46.0	70	37.0	3.1	30.3–42.5	1.1224	0.088
RPE										
Fovea	64	16.9	2.1	14.2–23.1	70	17.3	1.8	14.0–22.9	−0.3441	0.425
Pericentral ring	64	17.4	2.2	12.8–22.0	70	18.7	2.3	14.7–23.7	−0.9706	0.063
Peripheral ring	64	19.5	2.8	12.5–23.7	70	20.7	2.1	16.4–24.0	−0.9117	0.113
Total foveal RT	64	233.2	18.3	198.2–279.4	70	244.4	19.3	208.5–279.7	−11.2368	**0.012**
Total pericentral RT	64	316.9	16.5	283.4–348.8	70	319.3	14.1	287.1–345.1	−5.0431	0.162
Total peripheral RT	64	285.5	16.0	248.2–317.5	70	284.4	12.3	258.3–310.7	−0.8588	0.798
Peripapillary RNFL	63	112.1	15.8	81.0–143.9	67	111.2	9.5	91.4–129.8	0.8840	0.772

P values derived from multivariable linear mixed model and adjusted for age, sex, OCT quality factor, and spherical equivalent. *P* values in bold are $P < 0.05$. SD, standard deviation; *nr*, number of patients; *n*, number of eyes; GCL, ganglion cell layer; IPL, inner plexiform layer; INL, inner nuclear layer; OPL, outer plexiform layer; OSL, outer segment layer; RPE, retinal pigment epithelium; RT, retinal thickness.

method for evaluating retinal function is mf-ERG, but it requires adequate cooperation and can therefore be challenging to perform in children. Lastly, we did not measure peripapillary RNFL thickness in quadrants; therefore, it is possible that there were quadrantal changes in RNFL thickness in our patients while the average peripapillary RNFL thickness was not different between the two groups.

In summary, our findings indicate that HIV-infected children have a thinner foveal retinal thickness compared to matched controls while having comparable peripapillary RNFL thickness and visual function outcomes. Our results do not confirm the results of Moschos et al.[22,23]; however, they are in accordance with some recent studies in HIV-infected adults observing similar average peripapillary RNFL thickness between patients and controls,[1,9] and little difference in CS.[7,9] A novel finding in our study is the decrease in foveal thickness in the group of HIV-infected children; the clinical significance of this is yet unclear, since both VA and visual function were adequate. We postulate that HIV infection may disturb foveal maturation, leading to a thinner fovea. Although our results do not support the presence of a HIV-neuroretinal disorder, it is also possible that retinal (neuro)-degeneration will occur at a later time in patients' lives. The long-term effects of HIV infection on the retina are unknown, and as life expectancy of HIV-infected patients is increasing with the global rollout of cART, vision loss might become more prevalent and symptomatic with time. Therefore, longitudinal studies are warranted to investigate the effect of chronic HIV infection and long-term cART on the retinal structure and visual function of both HIV-infected adults and children.

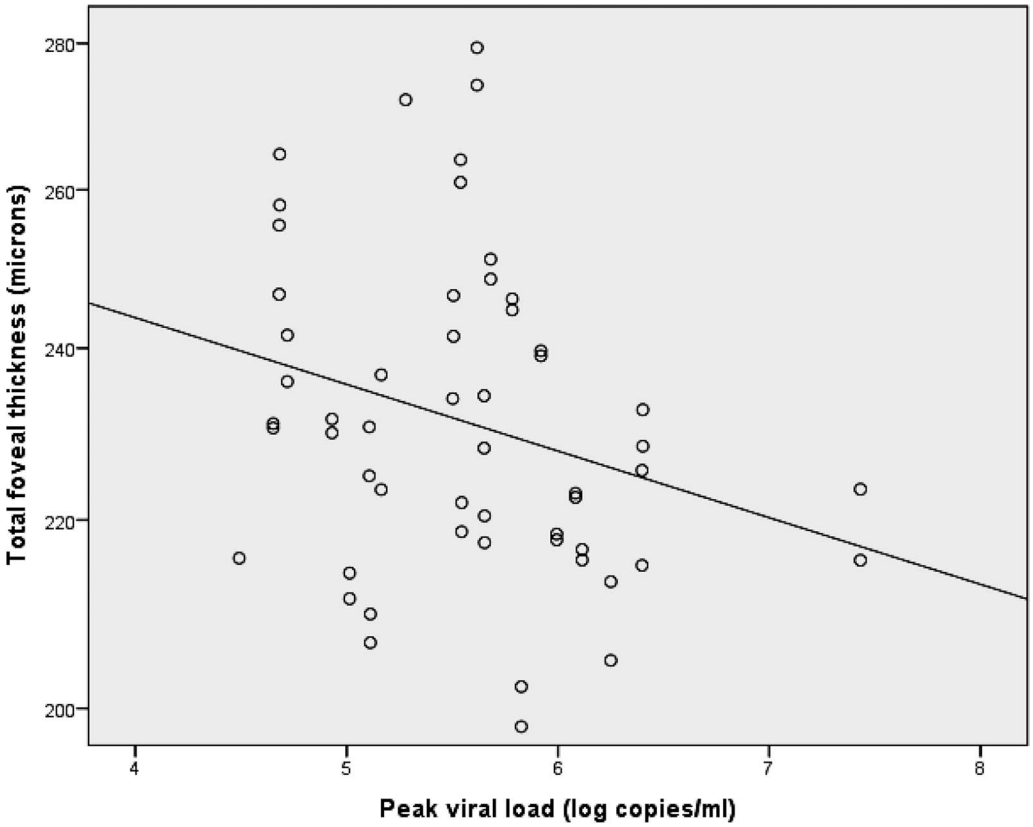

FIGURE 2. Correlation between total foveal thickness and peak HIV viral load.

Acknowledgments

Supported by Global Ophthalmology Awards Program 2012, Bayer HealthCare and the Emma Foundation (Grant 11.001).

Disclosure: **N. Demirkaya**, None; **S. Cohen**, None; **F.W.N.M. Wit**, None; **M.D. Abramoff**, IDx LLC (S), P; **R.O. Schlingemann**, Novartis (S); **T.W. Kuijpers**, None; **P. Reiss**, Gilead Sciences (S), Janssen Pharmaceutica (S); **D. Pajkrt**, None; **F.D. Verbraak**, Bayer HealthCare (F), Bayer NL (S), Novartis NL (S)

References

1. Arantes TE, Garcia CR, Tavares IM, Mello PA, Muccioli C. Relationship between retinal nerve fiber layer and visual field function in human immunodeficiency virus-infected patients without retinitis. *Retina*. 2012;32:152–159.
2. Falkenstein I, Kozak I, Kayikcioglu O, et al. Assessment of retinal function in patients with HIV without infectious retinitis by multifocal electroretinogram and automated perimetry. *Retina*. 2006;26:928–934.
3. Falkenstein IA, Bartsch DU, Azen SP, Dustin L, Sadun AA, Freeman WR. Multifocal electroretinography in HIV-positive patients without infectious retinitis. *Am J Ophthalmol*. 2008; 146:579–588.
4. Faria E, Arantes TE, Garcia CR, Mello PA, Muccioli C. Structural and functional assessment in HIV-infected patients using optical coherence tomography and frequency-doubling technology perimetry. *Am J Ophthalmol*. 2010;149:571–576.
5. Freeman WR, Van Natta ML, Jabs D, et al. Vision function in HIV-infected individuals without retinitis: report of the Studies of Ocular Complications of AIDS Research Group. *Am J Ophthalmol*. 2008;145:453–462.
6. Goldbaum MH, Falkenstein I, Kozak I, et al. Analysis with support vector machine shows HIV-positive subjects without infectious retinitis have mfERG deficiencies compared to normal eyes. *Trans Am Ophthalmol Soc*. 2008;106:196–204.
7. Kalyani PS, Holland GN, Fawzi AA, Arantes TE, Yu F, Sadun AA. Association between retinal nerve fiber layer thickness and abnormalities of vision in people with human immunodeficiency virus infection. *Am J Ophthalmol*. 2012;153:734–742, 742.ei.
8. Kozak I, Sample PA, Hao J, et al. Machine learning classifiers detect subtle field defects in eyes of HIV individuals. *Trans Am Ophthalmol Soc*. 2007;105:111–118.
9. Pathai S, Lawn SD, Weiss HA, Cook C, Bekker LG, Gilbert CE. Retinal nerve fibre layer thickness and contrast sensitivity in HIV-infected individuals in South Africa: a case-control study. *PLoS One*. 2013;8:e73694.
10. Shah KH, Holland GN, Yu F, Van NM, Nusinowitz S. Contrast sensitivity and color vision in HIV-infected individuals without infectious retinopathy. *Am J Ophthalmol*. 2006;142:284–292.
11. Dadgostar H, Holland GN, Huang X, et al. Hemorheologic abnormalities associated with HIV infection: in vivo assessment of retinal microvascular blood flow. *Invest Ophthalmol Vis Sci*. 2006;47:3933–3938.
12. Dejaco-Ruhswurm I, Kiss B, Rainer G, et al. Ocular blood flow in patients infected with human immunodeficiency virus. *Am J Ophthalmol*. 2001;132:720–726.
13. Furrer H, Barloggio A, Egger M, Garweg JG. Retinal microangiopathy in human immunodeficiency virus infection is related to higher human immunodeficiency virus-1 load in plasma. *Ophthalmology*. 2003;110:432–436.
14. Gangaputra S, Kalyani PS, Fawzi AA, et al. Retinal vessel caliber among people with acquired immunodeficiency syndrome: relationships with disease-associated factors and mortality. *Am J Ophthalmol*. 2012;153:434–444.

15. Kim A, Dadgostar H, Holland GN, et al. Hemorheologic abnormalities associated with HIV infection: altered erythrocyte aggregation and deformability. *Invest Ophthalmol Vis Sci*. 2006;47:3927–3932.
16. Pathai S, Weiss HA, Lawn SD, et al. Retinal arterioles narrow with increasing duration of anti-retroviral therapy in HIV infection: a novel estimator of vascular risk in HIV? *PLoS One*. 2012;7:e51405.
17. Tan PB, Hee OK, Cheung C, et al. Retinal vascular parameter variations in patients with human immunodeficiency virus. *Invest Ophthalmol Vis Sci*. 2013;54:7962–7967.
18. Kaul M, Garden GA, Lipton SA. Pathways to neuronal injury and apoptosis in HIV-associated dementia. *Nature*. 2001;410:988–994.
19. Kaul M, Lipton SA. Mechanisms of neuroimmunity and neurodegeneration associated with HIV-1 infection and AIDS. *J Neuroimmune Pharmacol*. 2006;1:138–151.
20. Tenhula WN, Xu SZ, Madigan MC, Heller K, Freeman WR, Sadun AA. Morphometric comparisons of optic nerve axon loss in acquired immunodeficiency syndrome. *Am J Ophthalmol*. 1992;113:14–20.
21. Xu H, Chen M, Forrester JV. Para-inflammation in the aging retina. *Prog Retin Eye Res*. 2009;28:348–368.
22. Moschos MM, Mostrou G, Psimenidou E, Spoulou V, Theodoridou M. Objective analysis of retinal function in HIV-positive children without retinitis using optical coherence tomography. *Ocul Immunol Inflamm*. 2007;15:319–323.
23. Moschos MM, Margetis I, Markopoulos I, Moschos MN. Optical coherence tomography and multifocal electroretinogram study in human immunodeficiency virus-positive children without infectious retinitis. *Clin Exp Optom*. 2011;94:291–295.
24. Cohen S, Ter Stege JA, Geurtsen GJ, et al. Poorer cognitive performance in perinatally HIV-infected children as compared to healthy socioeconomically matched controls. *Clin Infect Dis*. 2015;60:1111–1119.
25. Garvin MK, Abramoff MD, Kardon R, Russell SR, Wu X, Sonka M. Intraretinal layer segmentation of macular optical coherence tomography images using optimal 3-D graph search. *IEEE Trans Med Imaging*. 2008;27:1495–1505.
26. Garvin MK, Abramoff MD, Wu X, Russell SR, Burns TL, Sonka M. Automated 3-D intraretinal layer segmentation of macular spectral-domain optical coherence tomography images. *IEEE Trans Med Imaging*. 2009;28:1436–1447.
27. Bicknese L, Slot J. *Staat van de aandachtswijken*. Gemeente Amsterdam: Dienst Onderzoek en Statistiek; 2009:107–118. Project 9107.
28. Wechsler D. *Wechsler Adult Intelligence Scale Manual*. London: The Psychological Corporation; 2000.
29. Wechsler D. *Wechsler Intelligence Scale Manual*. London: The Psychological Corporation; 2002.
30. Comans-Bitter WM, de Groot R, van den Beemd R, et al. Immunophenotyping of blood lymphocytes in childhood. Reference values for lymphocyte subpopulations. *J Pediatr*. 1997;130:388–393.
31. Arditi A. Improving the design of the letter contrast sensitivity test. *Invest Ophthalmol Vis Sci*. 2005;46:2225–2229.
32. Dougherty BE, Flom RE, Bullimore MA. An evaluation of the Mars Letter Contrast Sensitivity Test. *Optom Vis Sci*. 2005;82:970–975.
33. Haymes SA, Roberts KF, Cruess AF, et al. The letter contrast sensitivity test: clinical evaluation of a new design. *Invest Ophthalmol Vis Sci*. 2006;47:2739–2745.
34. Thayaparan K, Crossland MD, Rubin GS. Clinical assessment of two new contrast sensitivity charts. *Br J Ophthalmol*. 2007;91:749–752.
35. Lanthony P. The desaturated panel D-15. *Doc Ophthalmol*. 1978;46:185–189.
36. Good GW, Schepler A, Nichols JJ. The reliability of the Lanthony Desaturated D-15 test. *Optom Vis Sci*. 2005;82:1054–1059.
37. Vingrys AJ, King-Smith PE. A quantitative scoring technique for panel tests of color vision. *Invest Ophthalmol Vis Sci*. 1988;29:50–63.
38. Frisen L. New, sensitive window on abnormal spatial vision: rarebit probing. *Vision Res*. 2002;42:1931–1939.
39. Salvetat ML, Zeppieri M, Parisi L, Brusini P. Rarebit perimetry in normal subjects: test-retest variability, learning effect, normative range, influence of optical defocus, and cataract extraction. *Invest Ophthalmol Vis Sci*. 2007;48:5320–5331.
40. Demirkaya N, van Dijk HW, van Schuppen SM, et al. Effect of age on individual retinal layer thickness in normal eyes as measured with spectral-domain optical coherence tomography. *Invest Ophthalmol Vis Sci*. 2013;54:4934–4940.
41. Ooto S, Hangai M, Tomidokoro A, et al. Effects of age, sex, and axial length on the three-dimensional profile of normal macular layer structures. *Invest Ophthalmol Vis Sci*. 2011;52:8769–8779.
42. Song WK, Lee SC, Lee ES, Kim CY, Kim SS. Macular thickness variations with sex, age, and axial length in healthy subjects: a spectral domain-optical coherence tomography study. *Invest Ophthalmol Vis Sci*. 2010;51:3913–3918.
43. Kashani AH, Zimmer-Galler IE, Shah SM, et al. Retinal thickness analysis by race, gender, and age using Stratus OCT. *Am J Ophthalmol*. 2010;149:496–502.
44. Rao HL, Kumar AU, Babu JG, Kumar A, Senthil S, Garudadri CS. Predictors of normal optic nerve head, retinal nerve fiber layer, and macular parameters measured by spectral domain optical coherence tomography. *Invest Ophthalmol Vis Sci*. 2011;52:1103–1110.
45. Huang J, Liu X, Wu Z, Sadda S. Image quality affects macular and retinal nerve fiber layer thickness measurements on fourier-domain optical coherence tomography. *Ophthalmic Surg Lasers Imaging*. 2011;42:216–221.
46. Samarawickrama C, Pai A, Huynh SC, Burlutsky G, Wong TY, Mitchell P. Influence of OCT signal strength on macular, optic nerve head, and retinal nerve fiber layer parameters. *Invest Ophthalmol Vis Sci*. 2010;51:4471–4475.
47. Lim MC, Hoh ST, Foster PJ, et al. Use of optical coherence tomography to assess variations in macular retinal thickness in myopia. *Invest Ophthalmol Vis Sci*. 2005;46:974–978.
48. Whitcup SM, Butler KM, Pizzo PA, Nussenblatt RB. Retinal lesions in children treated with dideoxyinosine. *N Engl J Med*. 1992;326:1226–1227.
49. Whitcup SM, Butler KM, Caruso R, et al. Retinal toxicity in human immunodeficiency virus-infected children treated with 2′,3′-dideoxyinosine. *Am J Ophthalmol*. 1992;113:1–7.
50. Whitcup SM, Dastgheib K, Nussenblatt RB, Walton RC, Pizzo PA, Chan CC. A clinicopathologic report of the retinal lesions associated with didanosine. *Arch Ophthalmol*. 1994;112:1594–1598.
51. Barteselli G, Chhablani J, Gomez ML, et al. Visual function assessment in simulated real-life situations in HIV-infected subjects. *PLoS One*. 2014;9:e97023.
52. Besada E, Shechtman D, Black G, Hardigan PC. Laser scanning confocal ophthalmoscopy and polarimetry of human immunodeficiency virus patients without retinopathy, under antiretroviral therapy. *Optom Vis Sci*. 2007;84:189–196.
53. Cheng S, Klein H, Bartsch DU, Kozak I, Marcotte TD, Freeman WR. Relationship between retinal nerve fiber layer thickness and driving ability in patients with human immunodeficiency virus infection. *Graefes Arch Clin Exp Ophthalmol*. 2011;249:1643–1647.

Investigative Ophthalmology & Visual Science

54. Gomez ML, Mojana F, Bartsch DU, Freeman WR. Imaging of long-term retinal damage after resolved cotton wool spots. *Ophthalmology*. 2009;116:2407–2414.
55. Holland GN, Kappel PJ, Van Natta ML, et al. Association between abnormal contrast sensitivity and mortality among people with acquired immunodeficiency syndrome. *Am J Ophthalmol*. 2010;149:807–816.
56. Kalyani PS, Fawzi AA, Gangaputra S, et al. Retinal vessel caliber among people with acquired immunodeficiency syndrome: relationships with visual function. *Am J Ophthalmol*. 2012; 153:428–433.
57. Kozak I, Bartsch DU, Cheng L, Kosobucki BR, Freeman WR. Objective analysis of retinal damage in HIV-positive patients in the HAART era using OCT. *Am J Ophthalmol*. 2005;139:295–301.
58. Kozak I, Bartsch DU, Cheng L, McCutchan A, Weinreb RN, Freeman WR. Scanning laser polarimetry demonstration of retinal nerve fiber layer damage in human immunodeficiency virus-positive patients without infectious retinitis. *Retina*. 2007;27:1267–1273.
59. Plummer DJ, Bartsch DU, Azen SP, Max S, Sadun AA, Freeman WR. Retinal nerve fiber layer evaluation in human immunodeficiency virus-positive patients. *Am J Ophthalmol*. 2001; 131:216–222.
60. Ho J, Sull AC, Vuong LN, et al. Assessment of artifacts and reproducibility across spectral- and time-domain optical coherence tomography devices. *Ophthalmology*. 2009;116: 1960–1970.
61. Vajzovic L, Hendrickson AE, O'Connell RV, et al. Maturation of the human fovea: correlation of spectral-domain optical coherence tomography findings with histology. *Am J Ophthalmol*. 2012;154:779–789.
62. Rutar T, Youm J, Porco T, et al. Ophthalmic manifestations of perinatally acquired HIV in a US cohort of long-term survivors. *Br J Ophthalmol*. 2015;99:650–653.
63. Jonnal RS, Kocaoglu OP, Zawadzki RJ, Lee SH, Werner JS, Miller DT. The cellular origins of the outer retinal bands in optical coherence tomography images. *Invest Ophthalmol Vis Sci*. 2014;55:7904–7918.

Investigative Ophthalmology & Visual Science